

# $^{124}\text{I}$ -MIBG: a new promising positron-emitting radiopharmaceutical for the evaluation of neuroblastoma

Angelina Cistaro<sup>1–3</sup>, Natale Quartuccio<sup>4</sup>, Federico Caobelli<sup>5</sup>, Arnoldo Piccardo<sup>6</sup>, Rosario Paratore<sup>7</sup>, Pietro Coppolino<sup>4</sup>, Alessandro Sperandeo<sup>7</sup>, Gaspare Arnone<sup>8</sup>, Umberto Ficola<sup>7</sup>

<sup>1</sup>Positron Emission Tomography Centre IRMET S.p.A., Euromedic Inc., Turin, Italy

<sup>2</sup>Coordinator of PET Pediatric AIMN InterGroup, Italy

<sup>3</sup>Associate researcher of Institute of Cognitive Sciences and Technologies, National Research Council, Rome, Italy

<sup>4</sup>Nuclear Medicine Unit, Department of Biomedical Sciences and of Morphologic and Functional Images, University of Messina, Italy

<sup>5</sup>Nuclear Medicine Unit, Hannover Medical School, Germany

<sup>6</sup>Nuclear Medicine Unit, Galliera Hospital, Genoa, Italy

<sup>7</sup>Department of Nuclear Medicine, La Maddalena Hospital, Palermo, Italy

<sup>8</sup>Nuclear Medicine Operating Unit, Civic Hospital, Palermo, Italy

The authors declare that they have no conflict of interest

[Received 1 I 2015; Accepted 31 III 2015]

## Abstract

Neuroblastoma is the most common extra-cranial solid tumor in pediatric patients. Despite the established role of  $^{123}\text{I}$ -MIBG and  $^{131}\text{I}$ -MIBG scintigraphy in this tumor, only limited data are available regarding the use of  $^{124}\text{I}$ -metaiodobenzylguanidine (MIBG) positron emission tomography (PET)/computed tomography (CT). We present our preliminary experience with  $^{124}\text{I}$ -MIBG PET/CT: two pediatric patients affected by neuroblastoma, who underwent  $^{124}\text{I}$ -MIBG PET/CT for pre-therapy distribution evaluation and restaging purposes. We aimed to evaluate whether  $^{124}\text{I}$ -MIBG PET/CT can detect as many or more neuroblastoma lesions than  $^{123}\text{I}/^{131}\text{I}$ -MIBG imaging. Our cases show promising results, although further validation and standardization of  $^{124}\text{I}$ -MIBG PET/CT are required.

**KEY words:** neuroblastoma,  $^{124}\text{I}$ -MIBG PET/CT, bone metastases,  $^{123}\text{I}$ -MIBG scan, radiometabolic therapy

Nuclear Med Rev 2015; 18, 2: 102–106

## Background

Neuroblastoma (NB) is the most common extra-cranial solid tumor in pediatric patients and originates from sympathetic cells derived from the neural crest. Bone and bone marrow metastases are quite common and, if present, result in a poor prognosis [1, 2]. Many studies have been reported the important role of  $^{123}\text{I}$ -Meta-iodobenzylguanidine (MIBG) at the time of first staging and at the evaluation of treatment response, especially after induction chemotherapy [3–5]. Moreover,  $^{123}\text{I}$ -MIBG scan is required when NB relapse is suspected and may establish the basis for the use of a targeted radionuclide therapy with  $^{131}\text{I}$ -MIBG [6]. The principal limitation of conventional nuclear medicine in neuroblastoma (mainly  $^{123}\text{I}$ -MIBG scan) is related to its relative low spatial resolution when compared with other radiological and

functional techniques such as CT, MRI and PET, similarly to what happens in other pediatric tumors [7–13].

MIBG labeled with  $^{124}\text{I}$ , a positron emitting isotope suitable for PET imaging, got increased interest in clinical practice [14–17]. The target of this radiocompound should be the capability of binding noradrenalin receptors as it happens with  $^{123}\text{I}$ -MIBG, but with a higher image quality and sensitivity granted by PET hardware [14]. However, limited data exist about the diagnostic accuracy of  $^{124}\text{I}$ -MIBG PET in NB.

We present the preliminary experience of the PET Pediatric AIMN (Italian Association of Nuclear Medicine) InterGroup with  $^{124}\text{I}$ -MIBG PET/CT in two pediatric patients diagnosed with neuroblastoma in order to highlight the improvement in diagnostic accuracy provided by  $^{124}\text{I}$ -MIBG PET/CT compared to the conventional imaging work-up assessing whether  $^{124}\text{I}$ -MIBG PET/CT could detect as many or more neuroblastoma lesions than  $^{123}\text{I}/^{131}\text{I}$ -MIBG imaging.

## Case series

### Case 1. Taking advantage of the better spatial resolution of $^{124}\text{I}$ -MIBG PET/CT

Patient No. 1 (10-year-old female) came to our observation with diagnosis of poorly differentiated abdominal neuroblastoma — stage

Correspondence to: Angelina Cistaro, MD,  
Positron Emission Tomography Centre IRMET S.p.A.  
Euromedic Inc.  
V. O. Vigliani 89/A, 10138 Turin, Italy  
Tel +39 01 13 160 159  
Fax +39 01 13 160 828  
E-mail: a.cistaro@irmet.com

III — with involvement of the left kidney and the homolateral adrenal gland. The patient had undergone neoadjuvant chemotherapy (cisplatin, etoposide and VP 16) before radical resection of the large abdominal mass. One year after surgery, the patient was referred for  $^{131}\text{I}$ -MIBG therapy (dose: 10 GBq) for a pulmonary relapse detected by a computed tomography (CT) exam. The  $^{123}\text{I}$ -MIBG pre-therapy and the  $^{131}\text{I}$ -post-therapy whole body scans depicted a single focal round-shaped uptake in the right lung. A week later, the child was proposed to scan with the experimental radiopharmaceutical  $^{124}\text{I}$ -MIBG for compassionate use, regulated by Legislative Decree No. 219/2006. After receiving written consent from the parents, the patient was evalu-

ated by PET/CT at 24h and 48h after the administration of 50 MBq of  $^{124}\text{I}$ -MIBG (radiochemical purity > 95%) (Fig. 1). The PET/CT study (Fig. 2) confirmed the finding detected by both  $^{123}\text{I}$ -MIBG scintigraphy and  $^{131}\text{I}$ -post-therapy whole body scan allowing a better characterization and localization of the finding in the basis of the right lung.

Afterwards, the patient underwent metastasectomy and the disease had a favorable course confirmed by a subsequent  $^{123}\text{I}$ -MIBG scintigraphy and a chest CT performed three and six months later, respectively. Nevertheless, the patient developed lumbar pain and signs of paraparesis a few months later, and a whole body CT with contrast medium revealed diffuse metastases to both lungs, abdominal lymph nodes and the fifth lumbar vertebra. Therefore the patient was referred for a second course of  $^{131}\text{I}$ -MIBG therapy. The  $^{131}\text{I}$ -MIBG post-therapy whole body scan (Fig. 3) was able to highlight all the lesions demonstrated by the CT scan, but pre-therapy  $^{124}\text{I}$ -MIBG PET/CT yielded a very good definition of the extent of disease (Fig. 4), demonstrating also the involvement of the medullary canal by the lesion located in the L3 vertebra, explaining the origin of the symptomatology of the patient, and revealed faint foci in L1, L4, L5 and sacrum (Fig. 5). On the basis of the clinical condition and imaging findings, the patient underwent a further treatment with  $^{131}\text{I}$ -MIBG, with a delivered dose of 10 GBq (270 mCi).

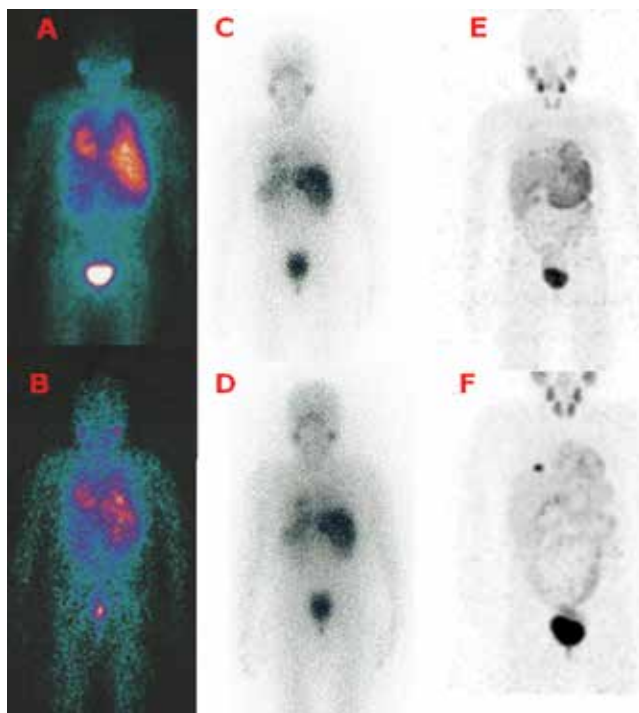


**Figure 1A–F.**  $^{124}\text{I}$ -MIBG planar images (A, B): posterior images, after 4 h (A) and 24 h (B) from radiopharmaceutical intravenous administration, documenting a lesion in the posterior region of the right pulmonary basis.  $^{131}\text{I}$ -MIBG post-therapy scan (C, D): anterior images, acquired 24 h (C) and 48 h (D) after injection. Uptake in the right lung is consistent with pulmonary recurrence.  $^{124}\text{I}$ -MIBG Maximum Intensity Projection (MIP) images after 24h (E) and 48h (F) show the same finding

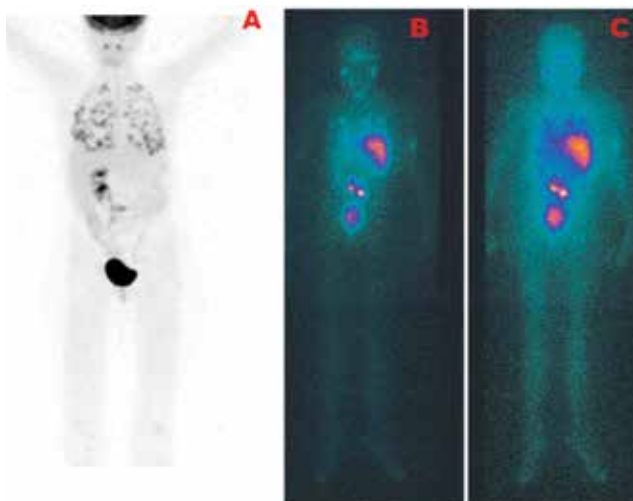


**Figure 3A–C.** Multiple pulmonary lesions evidenced by the  $^{124}\text{I}$ -MIBG PET/CT Maximum Intensity Projection (MIP) image (A) and the posterior views of  $^{131}\text{I}$ -MIBG post-therapy scan acquired 24 h (B) and 48 h (C) after injection

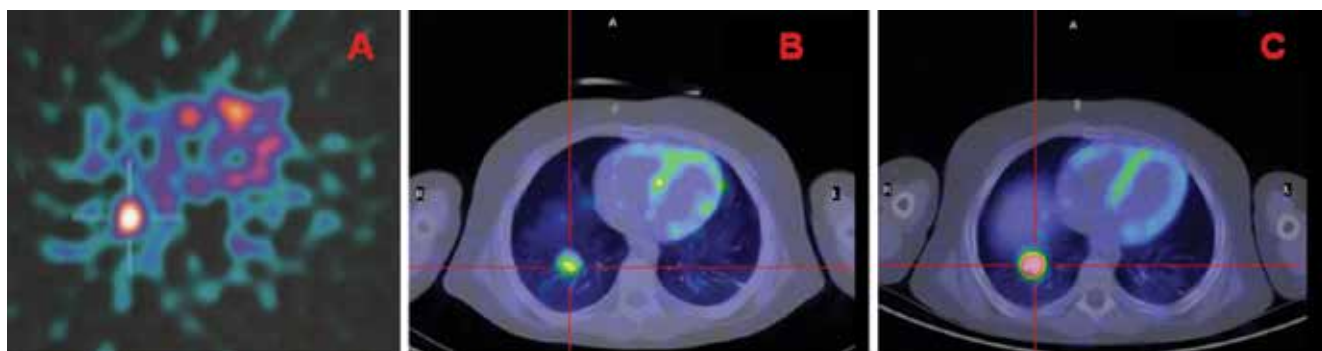


**Figure 2A–C.** Axial  $^{124}\text{I}$ -MIBG 24 h-SPECT image (A) and PET/CT fusion images taken at 24h (B) and 48h (C) documented the pulmonary lesion in the right lower pulmonary lobe. Of note the increased uptake over the time in the  $^{124}\text{I}$ -MIBG PET/CT images

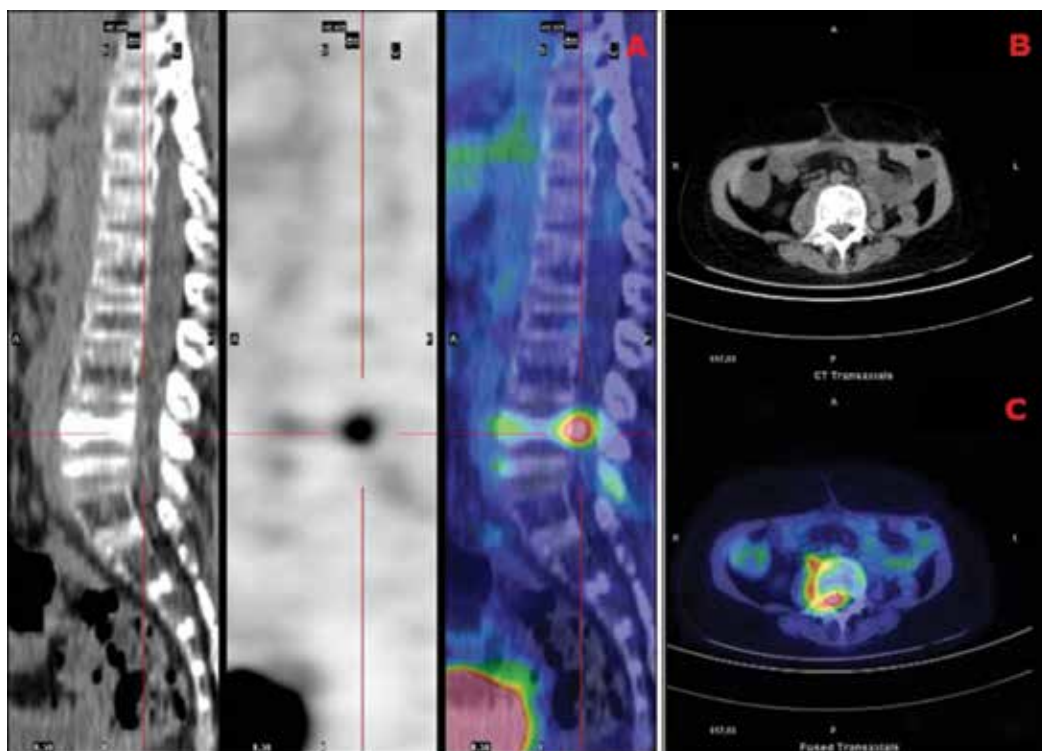


**Figure 4A.** Sagittal CT,  $^{124}\text{I}$ -MIBG PET and fused PET/CT images; **B.** Axial co-registered CT image at the level of the third lumbar vertebra; **C.** Axial  $^{124}\text{I}$ -MIBG PET/CT view of L3.  $^{124}\text{I}$ -MIBG PET/CT shows the same metastatic involvement of L3, as shown in figure 3 but with a dramatically improved definition, demonstrating the intracanal and the extra canal components of the lesion

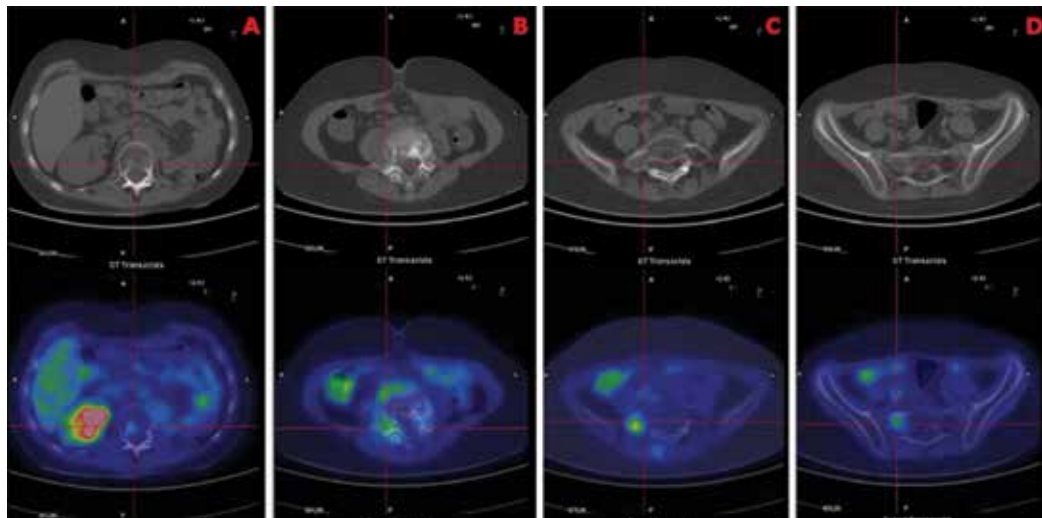


**Figure 5A–D.** Multiple metastatic lesions in patient No. 1 highlighted by  $^{124}\text{I}$ -MIBG PET/CT: L1 (A), L4 (B), L5 (C) and sacrum (D)

### **Case 2. Depiction of all metastatic sites in one single full-body exam**

Patient No. 2 was a 6-year-old boy with left adrenal gland neuroblastoma (stage IV) diagnosed when he was 1-year-old. The pathologic history had showed persistent bone disease involvement although the patient had already been treated with surgery, radiotherapy, chemotherapy and auto-transplantation over the years. After performing a follow-up  $^{123}\text{I}$ -MIBG scintigraphy in another center for restaging purposes, he was referred to our department to receive

a course of 9.9 GBq (270 mCi)  $^{131}\text{I}$ -MIBG. The  $^{131}\text{I}$ -MIBG post-therapy scan showed diffuse osseous disease (Fig. 6A, B) including the skull, the left scapula, several vertebrae, the right and left iliac bones, the ischiatic spine, the proximal part of the left tibia and the bone marrow canal of the right femur. After gaining informed consent from the patient,  $^{124}\text{I}$ -MIBG PET/CT was also performed for compassionate use and was able to visualize the same lesions as detected by the planar scintigraphy with  $^{131}\text{I}$ -MIBG (Fig. 6C–F) clearly providing images with better spatial resolution in all the bone districts.

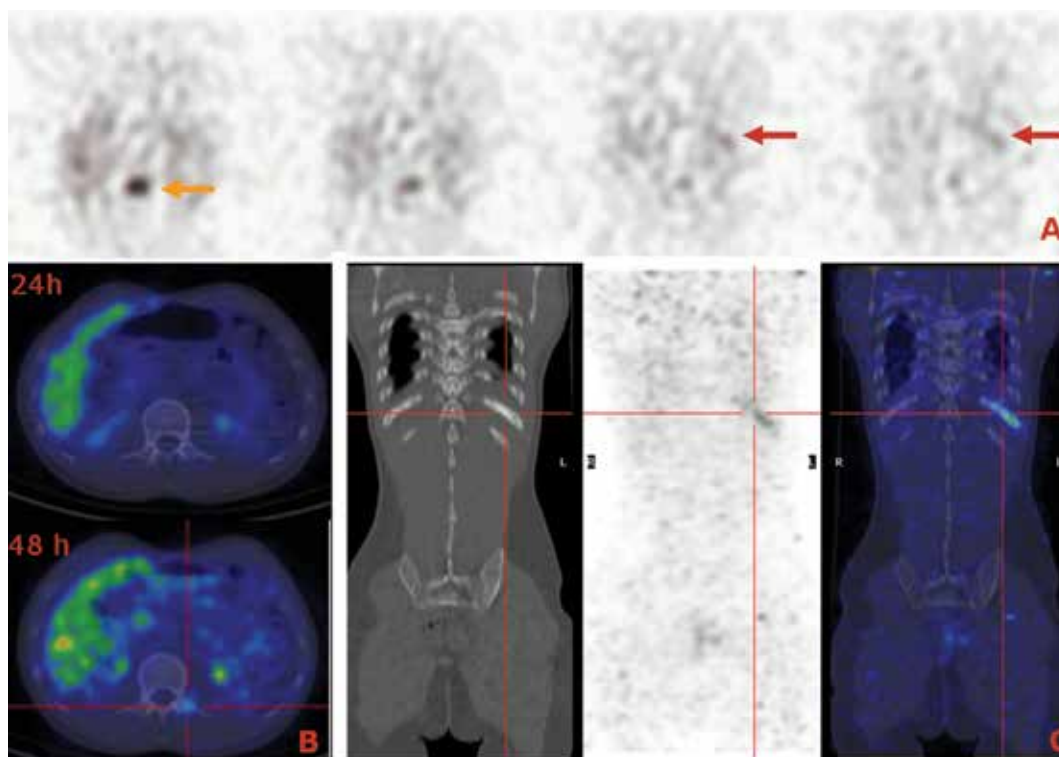


**Figure 6A–F.**  $^{131}\text{I}$ -MIBG post-therapy total body scan, anterior (A) and posterior (B) images: scintigraphic pattern consistent with multiple bone metastases (some of the lesions are evidenced by arrows: skull, pelvis and femur).  $^{124}\text{I}$ -MIBG PET/CT was also performed and was able to visualize the same number of metastases. Axial  $^{124}\text{I}$ -MIBG PET/CT fusion images showing some of the metastatic lesions with a dramatically improved definition; C. Skull; D–E. Pelvis; F. Right femur (an involvement of the left femur is also evident)

## Discussion

Although MIBG, radiolabeled with  $^{123}\text{I}$ , has high sensitivity (around 90%) and specificity close to 100% in the diagnosis of neuroblastoma [17], nevertheless an important role of labeled MIBG is also prospectively to evaluate the feasibility of  $^{131}\text{I}$ -MIBG radiometabolic therapy, which can be an additional therapeutic option in case of disseminated metastatic disease in which tumor cells have retained the capability of concentrating MIBG [6].

From this point of view,  $^{124}\text{I}$ -MIBG PET/CT represents a potential method to estimate radiation dose to normal organs, as well as tumors, prior to  $^{131}\text{I}$ -MIBG treatment and provide a more accurate quantification of tracer distribution because of its favorable characteristics, such as full-body tomographic capability from PET and a similar half-life (4.2 days) to  $^{131}\text{I}$  (8.02 days) [15].

Despite this important aspect, only few reports published in literature regarded the use of  $^{124}\text{I}$ -MIBG in adult patients with neural crest tumors [14, 16] and, to the best of our knowledge, only one child with neuroblastoma has been studied with  $^{124}\text{I}$ -MIBG PET/CT so far [18], providing data on dosimetry. Organ-absorbed doses for the salivary glands, heart wall and liver were 98.0 Gy, 36.5 Gy, and 34.3 Gy, respectively, whereas tumor-absorbed dose range was 143.9–1,641.3 Gy [18].

Many other studies investigated the role of PET/CT using other tracers such as  $^{18}\text{F}$ -DOPA [7, 19],  $^{68}\text{Ga}$ -labelled somatostatin analogues and  $^{18}\text{F}$ -FDG in patients with neuroblastoma [20]. Anyway, although these tracers can provide an excellent diagnostic accuracy in patients affected by neuroblastoma, nevertheless the labeled

pharmaceutical has a metabolic behavior which is similar but not equal to iodine-labeled MIBG.

In our series, we investigated if  $^{124}\text{I}$ -MIBG PET/CT could be considered a valuable tool in the diagnostic work-up of pediatric patient with advanced neuroblastoma.

From our experience,  $^{124}\text{I}$ -MIBG PET/CT provides high-resolution images and may offer valuable information regarding the extension of the lesion and the involvement of different types of tissue, addressing the most appropriate clinical management between surgical treatment and medical therapy [21]. In the present study, with the limit of lack of SPECT/CT, we could compare in our patients images obtained with  $^{123}\text{I}$ -MIBG scintigraphy,  $^{131}\text{I}$ -MIBG scintigraphy and with  $^{124}\text{I}$ -MIBG PET/CT, with the latter providing the same information about the tumor location in the case of the single round-shaped pulmonary lesion (patient n. 1).

In patient No. 1, the first  $^{124}\text{I}$ -MIBG PET/CT not only confirmed the finding detected by both  $^{123}\text{I}$ -MIBG scintigraphy and  $^{131}\text{I}$ -MIBG post-therapy scan, but allowed a better characterization and localization of the finding in the basis of the right lung, helping the clinical staff in the decision of performing a metastasectomy. Furthermore, the second  $^{124}\text{I}$ -MIBG PET/CT, performed in case No. 1, provided a very accurate definition of the extent of disease demonstrating the intracanal and the extra canal components of the lesion located at the level of L3 and detected a higher number of lesion (L1, L4, L5 and sacrum) in comparison to  $^{131}\text{I}$ -MIBG and CT. The findings of  $^{124}\text{I}$ -MIBG PET/CT were useful for the clinicians to link the symptomatology of the patient (lumbar pain and signs of paraparesis) to the pathologic involvement of the medullar canal.

Since metastatic spread of neuroblastoma may occur over the full length of the skeleton and since MIBG does not present uptake in the brain,  $^{124}\text{I}$ -MIBG gives excellent images of the skull and so is useful to detect secondary lesions in this anatomical region, which is a relatively frequent site of metastasis. Likewise,  $^{124}\text{I}$ -MIBG PET/CT should be performed in full body modality from the vertex of the skull to the feet.

A possible limitation in evaluating pediatric patients with  $^{124}\text{I}$ -MIBG PET/CT is the relatively higher radiation dose delivered (0.25 mSv/MBq) when compared to  $^{123}\text{I}$ -MIBG (0.019 mSv/MBq). Nevertheless, the improved characteristics of modern PET/CT scanners allow limiting the administered dose while maintaining an adequate image quality [22]. Moreover, the additional dose can be considered negligible by comparison if  $^{124}\text{I}$ -MIBG is performed as a pre-therapy evaluation tool before  $^{131}\text{I}$ -MIBG treatment.

Although there is lack of information in literature, this preliminary experience shows promising results for  $^{124}\text{I}$ -MIBG PET/CT; anyway, a large validation and a standardization of the technique is needed, such as for the optimal timing of  $^{124}\text{I}$ -MIBG PET imaging acquisition.

Multicenter investigations would be desirable, in order to foster the possible role of this technique in evaluating patients with neuroblastoma. At present, we could at least suggest to perform a  $^{124}\text{I}$ -MIBG PET/CT as a pre-therapy examination, given the high diagnostic accuracy demonstrated by our cases, and for restaging, especially when doubtful findings are evidenced by scintigraphic imaging with  $^{123}\text{I}$  or  $^{131}\text{I}$ -MIBG.

## References

1. Matthay KK, Shulkin B, Ladenstein R et al. Criteria for evaluation of disease extent by  $^{123}\text{I}$ -metaiodobenzylguanidine scans in neuroblastoma: a report for the International Neuroblastoma Risk Group (INRG) Task Force. *Br J Cancer* 2010; 102: 1319–1326.
2. Piccardo A, Lopci E, Conte M et al. PET/CT imaging in neuroblastoma. *Q J Nucl Med Mol Imaging* 2013; 57: 29–39.
3. Jacobson AF, Deng H, Lombard J, Lessig HJ, Black RR.  $^{123}\text{I}$ -Meta-iodobenzylguanidine scintigraphy for the detection of neuroblastoma and pheochromocytoma: results of a meta-analysis. *J Clin Endocrinol Metab* 2010; 95: 2596–606.
4. Matthay KK, Edeline V, Lumbroso J et al. Correlation of early metastatic response by  $^{123}\text{I}$ -metaiodobenzylguanidine scintigraphy with overall response and event-free survival in stage IV Neuroblastoma. *J Clin Oncol* 2003; 21: 2486–2491.
5. Sharp SE, Shulkin BL, Gelfand MJ, Salisbury S, Furman WL.  $^{123}\text{I}$ -MIBG scintigraphy and  $^{18}\text{F}$ -FDG PET in neuroblastoma. *J Nucl Med* 2009; 50: 1237–1243.
6. Taggart D, Dubois S, Matthay KK. Radiolabeled metaiodobenzylguanidine for imaging and therapy of neuroblastoma. *Q J Nucl Med Mol Imaging* 2008; 52: 403–418.
7. Lopci E, Piccardo A, Nanni C et al.  $^{18}\text{F}$ -DOPA PET/CT in neuroblastoma: comparison of conventional imaging with CT/MR. *Clin Nucl Med* 2012; 37: e73–e78.
8. Piccardo A, Lopci E, Conte M et al. Comparison of  $^{18}\text{F}$ -dopa PET/CT and  $^{123}\text{I}$ -MIBG scintigraphy in stage 3 and 4 neuroblastoma: a pilot study. *Eur J Nucl Med Mol Imaging* 2012; 39: 57–71.
9. Bombardieri E, Coliva A, Maccauro M et al. Imaging of neuroendocrine tumours with gamma-emitting radiopharmaceuticals. *Q J Nucl Med Mol Imaging* 2010; 54: 3–15.
10. Skanjeti A, Guerra L, Cistaro A.  $^{18}\text{F}$ -FDG-PET/CT in pediatric lymphoma. In: Cistaro A (ed.). *Atlas of PET/CT in pediatric patients*. Springer, Milan 2014: 39–59.
11. Quartuccio N, Cistaro A. Primary bone tumors. In: Cistaro A (ed.). *Atlas of PET/CT in pediatric patients*. Springer, Milan 2014: 67–86.
12. Cistaro A, Fania P, Valentini MC.  $^{18}\text{F}$ -FDG in the imaging of brain tumors In: Cistaro A (ed.). *Atlas of PET/CT in pediatric patients*. Springer, Milan 2014: 165–179.
13. Papathanasiou ND, Gaze MN, Sullivan K et al.  $^{18}\text{F}$ -FDG PET/CT and  $^{123}\text{I}$ -metaiodobenzylguanidine imaging in high-risk neuroblastoma: diagnostic comparison and survival analysis. *J Nucl Med* 2011; 52: 519–525.
14. Ott RJ, Tait D, Flower MA, Babich JW, Lambrecht RM. Treatment planning for  $^{131}\text{I}$ -mIBG radiotherapy of neural crest tumours using  $^{124}\text{I}$ -mIBG positron emission tomography. *Br J Radiol* 1992; 65: 787–791.
15. Lee CL, Wahnische H, Sayre GA et al. Radiation dose estimation using preclinical imaging with  $^{124}\text{I}$ -metaiodobenzylguanidine (MIBG) PET. *Med Phys* 2010; 37: 4861–4867.
16. Hartung-Knemeyer V, Rosenbaum-Krumme S, Buchbender C et al. Malignant pheochromocytoma imaging with  $^{124}\text{I}$ -mIBG PET/MR. *J Clin Endocrinol Metab* 2012; 97: 3833–3834.
17. Boubaker A, Bischof Delaloye A. MIBG scintigraphy for the diagnosis and follow-up of children with neuroblastoma. *Q J Nucl Med Mol Imaging* 2008; 52: 388–402.
18. Huang SY, Bolch WE, Lee C et al. Patient-specific dosimetry using pretherapy  $^{124}\text{I}$ -m-iodobenzylguanidine ( $^{124}\text{I}$ -mIBG) dynamic PET/CT imaging before  $^{131}\text{I}$ -mIBG targeted radionuclide therapy for neuroblastoma. *Mol Imaging Biol*. 2014; 17: 284–294. doi: 10.1007/s11307-014-0783-7.
19. Lu MY, Liu YL, Chang HH et al.; National Taiwan University Neuroblastoma Study Group. Characterization of neuroblastic tumors using  $^{18}\text{F}$ -FDOPA PET. *J Nucl Med* 2013; 54: 42–49.
20. Mueller WP, Coppenrath E, Pfluger T. Nuclear medicine and multimodality imaging of pediatric neuroblastoma. *Pediatr Radiol* 2013; 43: 418–427.
21. Seo Y, Gustafson WC, Dannoon SF et al. Tumor dosimetry using  $^{124}\text{I}$ -m-iodobenzylguanidine microPET/CT for  $^{131}\text{I}$ -m-iodobenzylguanidine treatment of neuroblastoma in a murine xenograft model. *Mol Imaging Biol* 2012; 14: 735–742.
22. Boellaard R, O'Doherty MJ, Weber WA et al. FDG PET and PET/CT: EANM procedure guidelines for tumour PET imaging: version 1.0 *Eur J Nucl Med Mol Imaging* 2010; 37: 181–200.